Caspian Journal of Mathematical Sciences (CJMS)
University of Mazandaran, Iran
http://cjms.journals.umz.ac.ir
https://doi.org/10.22080/cjms.2026.30896.1796
Caspian J Math Sci. **15**(2)(2026), 300-321 (Research Article)

Hybrid Neuro-Fuzzy and Artificial Neural Network Modeling of Radiative MHD Sisko Nanofluid Flow over Stretching and Shrinking Surfaces with Joule Heating and Viscous Dissipation

N Ramya[1], Farshid Mofidnakhaei [2]
[1] Department of Mathematics, Kongu Engineering College, Erode 638060, India. Email: jpramyamaths@gmail.com
[2] Department of Physics, Sar.C., Islamic Azad University, Sari, Iran. E-mail: Farshid.Mofidnakhaei@gmail.com

Abstract. A coupled numerical and intelligent modeling strategy is developed to analyze radiative magnetohydrodynamic flow of a non-Newtonian Sisko nanofluid over stretching and shrinking surfaces in the presence of Joule heating, nonlinear viscous dissipation, Brownian diffusion, thermophoresis, and motile microorganism transport. The mathematical formulation consists of boundary-layer equations governing momentum, thermal energy, solutal concentration, and microorganism density, incorporating Lorentz force effects and nonlinear shear-dependent viscosity. By employing suitable similarity transformations, the governing partial differential equations are reduced to a highly nonlinear system of ordinary differential equations and solved numerically using a boundary value approach. The numerical solutions reveal the existence of dual solution branches for shrinking surfaces, indicating bifurcation phenomena governed by viscous dissipation and stretching/shrinking

[1]Corresponding author: jpramyamaths@gmail.com
Received: 24 December 2025
Revised: 17 February 2026
Accepted: 17 March 2026
How to Cite: Ramya, N.; Mofidnakhaei, Farshid. Hybrid Neuro-Fuzzy and Artificial Neural Network Modeling of Radiative MHD Sisko Nanofluid Flow over Stretching and Shrinking Surfaces with Joule Heating and Viscous Dissipation. Casp.J. Math. Sci.,**15**(2)(2026), 300-321.

intensity. The computed datasets are subsequently utilized to construct Artificial Neural Network (ANN) and Adaptive Neuro-Fuzzy Inference System (ANFIS) surrogate models for accurate prediction of skin friction, heat transfer, mass transfer, and microorganism density rates. A close correspondence between numerical and intelligent predictions is observed, with correlation coefficients exceeding 0.99. The analysis demonstrates that Joule heating and viscous dissipation markedly elevate the thermal field while diminishing solutal and nanoparticle concentration levels, whereas magnetic interaction suppresses fluid motion and thickens the thermal boundary layer. The proposed hybrid numerical–intelligent framework provides an efficient and reliable tool for simulating complex nonlinear MHD nanofluid transport processes.

Keywords: Neural network, Sisko nanofluid, Stretching/Shrinking Surface, Thermal radiation, Viscous Dissipation.

2000 Mathematics subject classification: xxxx, xxxx; Secondary xxxx.

1. Introduction

Recent advances in non-Newtonian nanofluid research have increasingly focused on Sisko fluid models due to their ability to capture both shear-thinning and shear-thickening rheological behaviors encountered in complex industrial and biomedical flows. The integration of artificial intelligence with numerical simulations has emerged as a powerful framework for modeling such highly nonlinear transport phenomena under magnetohydrodynamic (MHD) and thermal effects.

Divya et al. [1] pioneered the application of hybrid artificial neural network and fuzzy inference modeling to unsteady Sisko trihybrid nanofluid flows, highlighting entropy generation mechanisms relevant to cancer therapy applications. Their findings demonstrated that neuro-fuzzy approaches significantly enhance predictive reliability in thermally sensitive biomedical systems. Building on ANN-based learning strategies, Ali et al. [2] employed the Levenberg–Marquardt back-propagation algorithm to predict heat transfer characteristics in MHD tangent hyperbolic nanofluid flows over stretching surfaces, confirming the robustness of ANN models in handling strong magnetic and viscous interactions.

Neural-network-driven investigations of Sisko nanofluid boundary-layer flows were further extended by Jyothi et al. [3], who analyzed coupled momentum and thermal transport under magnetic effects. Similarly, Mahanta and Sharma [4] examined different classes of non-Newtonian fluids over deformable melting surfaces, incorporating nonlinear radiation and velocity slip, and demonstrated that ANN frameworks effectively capture flow nonlinearity. Qureshi et al. [5] explored hybrid polymer/CNT nanofluid heat exchange across parallel plates, revealing the superior learning capability of neural networks in multi-component nanofluid systems.

The role of aggregation dynamics and entropy generation in Darcy–Forchheimer porous flows was investigated by Mahmood et al. [6] using ANN-based modeling, emphasizing irreversibility minimization under nonlinear thermal radiation. Magnetized Casson nanofluid flows with Soret and Dufour effects were numerically studied by Ramya and Deivanayaki [7, 8], elucidating the coupled heat and mass diffusion mechanisms under magnetic fields. Siddique et al. [9] incorporated fuzzy volume fraction concepts into ANN-based modeling of third-grade hybrid nanofluids, demonstrating improved accuracy under nonlinear radiation and heat generation. Islam et al. [10] employed CFD techniques to analyze extended tetra-hybrid Sisko nanofluid flow through stenosed arteries, revealing critical implications for biomedical transport systems.

Peristaltic transport phenomena in Sisko nanofluids were extensively examined by Bilal et al. [11], incorporating viscous dissipation, induced magnetic fields, and double-diffusive convection. Akram et al. [14] further analyzed magnetized peristaltic Sisko nanofluid flow in asymmetric channels, highlighting the combined effects of thermal radiation and slip. Raafat et al. [12] characterized thermal efficiency and entropy generation of Sisko nanofluids in parabolic trough solar collectors, comparing different carbon-based nanoparticles. Nisha and De [13] presented a comparative bioconvective analysis of di-, tri-, and tetra-hybrid Sisko nanofluids over porous cones and plates, emphasizing the influence of viscous dissipation, radiation, and chemical reactions.

Velocity slip and nonlinear stretching effects were addressed by Baral and Kumar [15], while Shaheen et al. [16] investigated MHD heat transfer in Sisko nanofluid flow through vertical endoscopic channels. Optimization-based hydrothermal analysis of Sisko nanofluids under magnetic fields was performed by Wang et al. [17]. Ramya and Deivanayaki [18] investigated the influence of thermal radiation on Casson nanofluid flow over an inclined stretching surface incorporating simultaneous heat and mass diffusion effects.The combined effects of thermophoresis and Brownian motion in Casson ternary hybrid nanofluids with gyrotactic microorganisms were explored by Ramya et al. [19]. Classical investigations on MHD stagnation-point flow [20] and radiative magneto-Sisko nanofluid flow with entropy analysis [21] further enriched the foundational understanding of Sisko fluid dynamics.

Microorganism-induced transport in Carreau nanofluids was reported by Ramya and Deivanayaki [22], while Muhiuddin et al. [23] examined Williamson fluid bioconvection over curved porous surfaces. The influence of homogeneous–heterogeneous reactions with Cattaneo–Christov heat flux in micropolar nanofluids was analyzed by Ramya et al. [24]. Additional studies addressed radiative and bioconvective Sisko nanofluid flows with variable conductivity and magnetic effects [25, 26, 27, 28, 29]. More recently, Adilakshmi et al. [30], Abbas et al. [31], Sohail et al. [32], Islam et al. [33], Bibi et al. [34], and Dadhich et al. [35] investigated advanced MHD Sisko nanofluid configurations incorporating radiation, diffusion, chemical reactions, and viscous dissipation. Joule heating and variable viscosity effects in curved and peristaltic channels were further analyzed by Tanveer et al. [36] and Hussein et al. [37]. Muhiuddin et al. [38] examined stagnation-point flow of a Sisko nanofluid over a stretching surface considering heat generation and nano-transport mechanisms, and analyzed the effects of rheological and thermal parameters on velocity, temperature, and concentration distributions. Ahmed et al. [39] investigated biomedical heat and mass transport in hybrid nanofluid flow with bioconvection and reactive species over an oscillatory curved porous surface, highlighting the influence of porosity variation and chemical reactions on thermal performance. Muhiuddin et al. [40] analyzed Williamson nanofluid flow over a porous curved stretching surface under homogeneous–heterogeneous reactions and bioconvection, discussing the impact of chemical and porous parameters on heat and microorganism transport. Noreen et al. [41] modeled bioconvective Casson nanofluid flow with activation energy and gyrotactic microorganisms over a curved surface with thermal radiation, emphasizing the effects of activation energy and radiation on flow behavior. Ramya and Deivanayaki [42] studied Casson nanofluid flow over a stretching surface embedded in a porous medium incorporating thermal radiation and particle diffusion effects, and evaluated their influence on heat and mass transfer rates. Sankari et al. [43] explored Williamson MHD nanofluid flow over a porous exponentially stretching sheet with bioconvective fluxes, focusing on magnetic field and porous medium effects on thermal and concentration characteristics.

Despite these extensive contributions, hybrid ANN–ANFIS modeling of radiative MHD Sisko nanofluid flow over stretching and shrinking surfaces with Joule heating and viscous dissipation remains largely unexplored, particularly in the context of dual-solution bifurcation behavior and statistical validation using Taylor diagrams. The present study aims to bridge this gap by developing a unified numerical–intelligent framework capable of accurately predicting and interpreting complex nonlinear transport phenomena.

2. Objectives

The primary objectives of this study are:

(1) To investigate the effects of stretching and shrinking surfaces on radiative MHD Sisko nanofluid flows incorporating Joule heating and viscous dissipation.
(2) To analyze the influence of key physical parameters—such as magnetic parameter, Prandtl number, Eckert number, and Sisko fluid parameters—on velocity, temperature, and nanoparticle concentration fields.
(3) To develop hybrid computational models using *Artificial Neural Networks (ANNs)* and *Adaptive Neuro-Fuzzy Inference Systems (ANFIS)* for predicting flow and thermal characteristics.
(4) To generate 3D parametric visualizations and surface plots to compare numerical results with ANN and ANFIS predictions, providing insight into dual solutions and bifurcation behavior.
(5) To evaluate the efficiency and accuracy of hybrid models by performing statistical error analyses, including RMSE, MAE, and R^2, for ANN and ANFIS predictions.
(6) To provide a framework for future applications of hybrid AI models in advanced thermal management, biomedical engineering, and industrial heat transfer systems involving non-Newtonian nanofluids.

Figure 1 presents the complete computational and intelligent modeling framework adopted in this study. The analysis begins with the formulation of governing equations for radiative magnetohydrodynamic Sisko nanofluid flow over stretching and shrinking surfaces, incorporating Joule heating, viscous dissipation, nanoparticle diffusion, and microorganism transport. Through similarity transformations, the governing partial differential equations are reduced to a system of highly nonlinear ordinary differential equations, which are solved numerically using MATLAB's `bvp4c` solver.

The numerical solutions serve as high-fidelity reference data for training intelligent surrogate models. A feedforward Artificial Neural Network (ANN) is first employed to capture global nonlinear trends in the flow and heat transfer characteristics. Subsequently, an Adaptive Neuro-Fuzzy Inference System (ANFIS) is developed to enhance local prediction accuracy by integrating fuzzy logic with neural learning. The

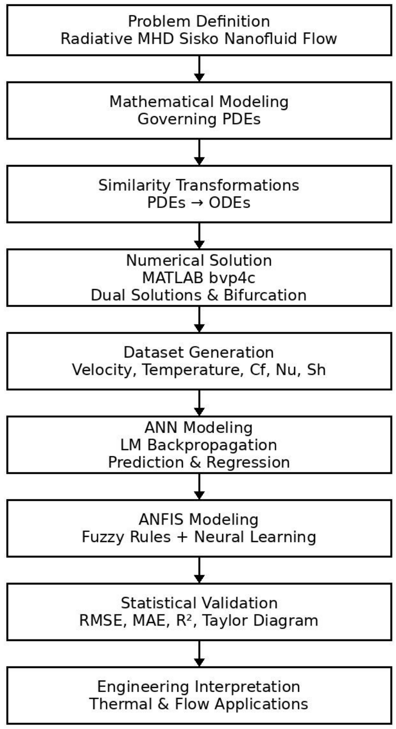

FIGURE 1. Methodological workflow of the present study illustrating the sequential integration of numerical modeling, ANN prediction, and ANFIS-based refinement for radiative MHD Sisko nanofluid flow with Joule heating and viscous dissipation.

predictive performance of both models is rigorously evaluated using statistical error metrics, including RMSE, MAE, and the coefficient of determination, along with Taylor diagram analysis. Finally, the validated hybrid framework is used to interpret the thermal and hydrodynamic behavior of the system for practical engineering applications.

3. Mathematical Formulation

In this study, we investigate the steady, incompressible, radiative magnetohydrodynamic (MHD) flow of a Sisko nanofluid over stretching and shrinking surfaces under the influence of Joule heating, viscous dissipation, and nanoparticle dynamics. The governing equations are formulated using boundary layer approximations, assuming a laminar flow regime.

3.1. Governing Equations.

- **Continuity Equation:**

$$\frac{\partial u}{\partial x} + \frac{\partial v}{\partial y} = 0, \tag{3.1}$$

  which ensures mass conservation in the boundary layer. Here, u and v are the velocity components along the x and y directions, respectively.

- **Momentum Equation:**

$$u\frac{\partial u}{\partial x}+v\frac{\partial u}{\partial y} = U_\infty\frac{dU_\infty}{dx}+\frac{a}{\rho_f}\frac{\partial^2 u}{\partial y^2}-\frac{b}{\rho_f}\frac{\partial}{\partial y}\Big[-\frac{\partial u}{\partial y}\Big]^n+\frac{\sigma B_0^2}{\rho_f}(U_\infty-u), \tag{3.2}$$

  where a and b are material parameters related to the Sisko fluid model, n is the non-Newtonian index, ρ_f is the fluid density, and B_0 is the applied magnetic field. The terms represent:
  (1) *Convective acceleration:* $u\frac{\partial u}{\partial x} + v\frac{\partial u}{\partial y}$
  (2) *Free stream acceleration:* $U_\infty\frac{dU_\infty}{dx}$
  (3) *Viscous contribution:* $\frac{a}{\rho_f}\frac{\partial^2 u}{\partial y^2}$
  (4) *Non-Newtonian stress effect:* $-\frac{b}{\rho_f}\frac{\partial}{\partial y}\left(-\frac{\partial u}{\partial y}\right)^n$
  (5) *Lorentz force due to magnetic field:* $\frac{\sigma B_0^2}{\rho_f}(U_\infty - u)$

- **Energy Equation:**

$$u\frac{\partial T}{\partial x} + v\frac{\partial T}{\partial y} = \alpha_m\frac{\partial^2 T}{\partial y^2} + \frac{\sigma B_0^2}{(\rho C_p)_f}(U_\infty - u)^2 + \frac{1}{(\rho C_p)_f}\left[a\left(\frac{\partial u}{\partial y}\right)^2 + b\left(-\frac{\partial u}{\partial y}\right)^{n+1}\right] + \frac{\tau D_B}{(\rho C_p)_f}\frac{\partial \phi}{\partial y}\frac{\partial T}{\partial y} + \frac{D_C}{(\rho C_p)_f}\frac{\partial^2 C}{\partial y^2} + \frac{Q_0}{(\rho C_p)_f}. \tag{3.3}$$

  This equation accounts for:
  (1) Thermal conduction: $\alpha_m\frac{\partial^2 T}{\partial y^2}$
  (2) Joule heating due to MHD: $\frac{\sigma B_0^2}{(\rho C_p)_f}(U_\infty - u)^2$
  (3) Viscous dissipation and non-Newtonian work: $\frac{1}{(\rho C_p)_f}[a(\partial u/\partial y)^2 + b(-\partial u/\partial y)^{n+1}]$

(4) Brownian motion: $\frac{\tau D_B}{(\rho C_p)_f}(\partial\phi/\partial y)(\partial T/\partial y)$
(5) Thermophoresis: $\frac{D_C}{(\rho C_p)_f}\partial^2 C/\partial y^2$
(6) Heat generation/absorption: $Q_0/(\rho C_p)_f$

- **Species Concentration Equation:**

$$u\frac{\partial C}{\partial x} + v\frac{\partial C}{\partial y} = D_S\frac{\partial^2 C}{\partial y^2} + D_T\frac{\partial^2 T}{\partial y^2}, \tag{3.4}$$

where C is the nanoparticle concentration, D_S is the Brownian diffusion coefficient, and D_T is the thermophoretic diffusion coefficient.

- **Motile Microorganism Equation:**

$$u\frac{\partial \phi}{\partial x} + v\frac{\partial \phi}{\partial y} = D_B\frac{\partial^2 \phi}{\partial y^2} + \frac{D_T}{T_\infty}\frac{\partial^2 T}{\partial y^2}, \tag{3.5}$$

which models the motile microorganism transport influenced by Brownian motion and thermophoresis.

3.2. **Boundary Conditions.** The physical constraints at the wall and far from the wall are given by:

$$\begin{aligned} &u = u_w = cx, \quad v = v_w, \quad T = T_w, \quad C = C_w, \quad \phi = \phi_w, \quad y = 0,\\ &u \to U_\infty, \quad v \to 0, \quad T \to T_\infty, \quad C \to C_\infty, \quad \phi \to \phi_\infty, \quad y \to \infty. \end{aligned} \tag{3.6}$$

These conditions represent the stretching/shrinking sheet with specified wall temperature, concentration, and microorganism density.

3.3. **Similarity Transformations.** To reduce the governing PDEs to ODEs, the following similarity transformations are introduced:

$$\begin{aligned} &u = u_w f'(\eta), \quad v = \dots,\\ &\eta = y\left(\frac{c^{2-n}}{b/\rho_f}\right)^{1/(n+1)} x^{(1-n)/(1+n)},\\ &\theta(\eta) = \frac{T - T_\infty}{T_w - T_\infty}, \quad S(\eta) = \frac{C - C_\infty}{C_w - C_\infty}, \quad \phi(\eta) = \frac{\phi - \phi_\infty}{\phi_w - \phi_\infty}. \end{aligned} \tag{3.7}$$

These transformations ensure that the flow variables are expressed in terms of the single similarity variable η, allowing for a boundary layer reduction.

3.4. **Transformed Nonlinear ODEs.** After applying the similarity transformations, the governing equations reduce to:

$$Af''' + n(-f'')^{n-1}f''' + \frac{2n}{n+1}f'f'' + \frac{d^2}{c^2} - f'^2 + M\left(\frac{d}{c} - f'\right) = 0, \tag{3.8}$$

$$\theta'' + \Pr\frac{2n}{n+1}f\theta' + \Pr M \mathrm{Ec}(1-f')^2 + \Pr\ \mathrm{Ec}\left[A(f'')^2 + (-f'')^{n+1}\right] + \Pr\ \mathrm{Nb}\theta'\phi' + \Pr\ \mathrm{Nt}(\theta')^2 + N_d S'' = 0, \tag{3.9}$$

$$S'' + \mathrm{Le}\ \Pr\frac{2n}{n+1}fS' + L_d\theta'' = 0, \tag{3.10}$$

$$\phi'' + \mathrm{Lb}\ \Pr\frac{2n}{n+1}f\phi' + \frac{Nt}{Nb}\theta'' = 0. \tag{3.11}$$

3.5. **Dimensionless Physical Quantities.**

$$C_f = \mathrm{Re}_b^{\frac{1}{n+1}}\left[f''(0) - (-f''(0))^n\right], \qquad \mathrm{Nu}_x = -\mathrm{Re}_b^{-\frac{1}{n+1}}\theta'(0),$$
$$\mathrm{Sh}_x = -\mathrm{Re}_b^{-\frac{1}{n+1}}S'(0), \qquad \mathrm{Sh}_{x,n} = -\mathrm{Re}_b^{-\frac{1}{n+1}}\phi'(0), \tag{3.12}$$

representing the skin friction coefficient, Nusselt number, and Sherwood numbers, respectively.

3.6. **First-Order System for Numerical Solution.** To employ numerical solvers such as `bvp4c`, we transform the above system into a first-order system:

$$y_1 = f, \quad y_2 = f', \quad y_3 = f'',$$
$$y_4 = \theta, \quad y_5 = \theta', \quad y_6 = S,$$
$$y_7 = S', \quad y_8 = \phi, \quad y_9 = \phi'.$$

The derivatives become:

$$y_1' = y_2, \qquad y_2' = y_3,$$
$$y_3' = \frac{y_2^2 - \frac{2n}{n+1}y_1y_3 - \frac{d^2}{c^2} - M(\frac{d}{c} - y_2)}{A + n(-y_3)^{n-1}},$$
$$y_5' = -\Pr\frac{2n}{n+1}y_1y_5 - \Pr M\mathrm{Ec}(1-y_2)^2 - \Pr\ \mathrm{Ec}[Ay_3^2 + (-y_3)^{n+1}] - \Pr\ \mathrm{Nb}y_5y_9 - \Pr\ \mathrm{Nt}y_5^2 - N_d y_7',$$
$$y_7' = -\mathrm{Le}\ \Pr\frac{2n}{n+1}y_1y_7 - L_d y_5',$$
$$y_9' = -\mathrm{Lb}\ \Pr\frac{2n}{n+1}y_1y_9 - \frac{Nt}{Nb}y_5'. \tag{3.13}$$

The boundary conditions in first-order form are:

$$y_1(0) = 0, \quad y_2(0) = \lambda, \quad y_4(0) = 1, \quad y_6(0) = 1, \quad y_8(0) = 1,$$
$$y_2(\infty) = 0, \quad y_4(\infty) = 0, \quad y_6(\infty) = 0, \quad y_8(\infty) = 0. \quad (3.14)$$

4. Results and Discussion

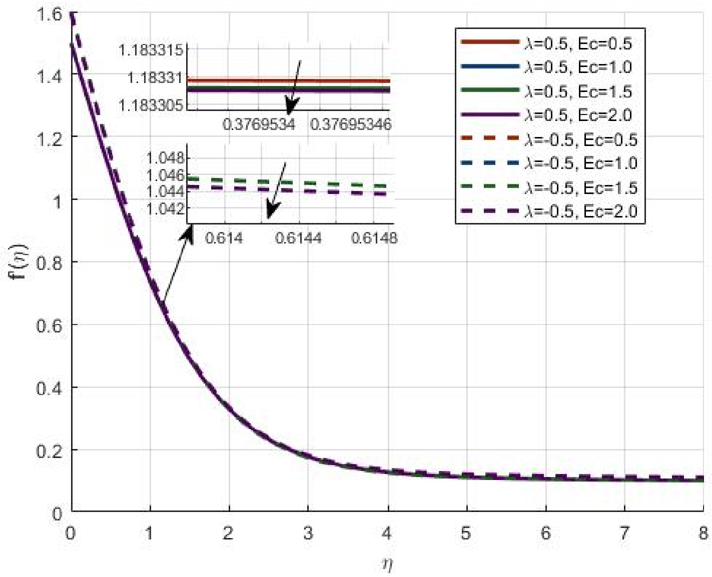

Figure 2. Influence of Eckert number (Ec) on the Velocity profile $\theta(\eta)$ for stretching ($\lambda = 0.5$) and shrinking ($\lambda = -0.5$) surfaces. Solid lines represent the first (stable) solution, while dashed lines correspond to the second (unstable) solution.

Figures 3–5 illustrate the influence of the Eckert number (Ec) on the temperature, solutal concentration, and nanoparticle concentration distributions for both stretching ($\lambda = 0.5$) and shrinking ($\lambda = -0.5$) surfaces. The Eckert number quantifies the conversion of kinetic energy into internal energy through viscous dissipation, which becomes particularly significant in high-speed and highly viscous non-Newtonian flows.

For the temperature field (Figure 3), an increase in Ec leads to a pronounced enhancement in $\theta(\eta)$ for both solution branches. Physically, higher viscous dissipation intensifies internal heat generation within the boundary layer, resulting in thicker thermal boundary layers. The effect

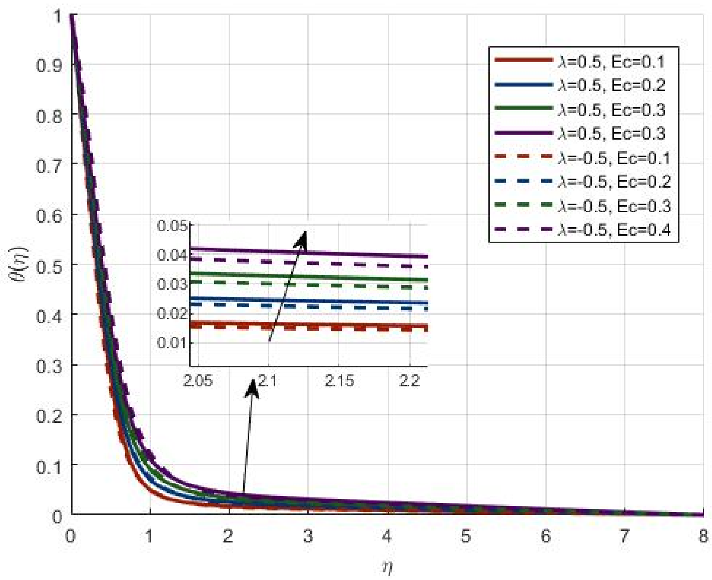

FIGURE 3. Influence of Eckert number (Ec) on the temperature profile $\theta(\eta)$ for stretching ($\lambda = 0.5$) and shrinking ($\lambda = -0.5$) surfaces. Solid lines represent the first (stable) solution, while dashed lines correspond to the second (unstable) solution.

is more prominent for the first (stable) solution, whereas the second solution exhibits comparatively weaker thermal diffusion, indicating its unstable nature.

Figure 4 depicts the variation of the solutal concentration profile with increasing Ec. It is observed that higher viscous heating reduces the solutal concentration within the boundary layer, as thermal agitation weakens concentration gradients. The presence of dual solutions is evident in the shrinking case, where the second solution displays lower concentration levels and a thinner solutal boundary layer, emphasizing bifurcation-induced sensitivity.

Similarly, the nanoparticle concentration profiles shown in Figure 5 demonstrate a decreasing trend with increasing Ec. Enhanced viscous dissipation accelerates thermal diffusion, which indirectly suppresses nanoparticle accumulation near the surface. The separation between the two solution branches becomes more noticeable in the shrinking regime, confirming the existence of multiple steady states.

The inset plots in all figures magnify regions where solution bifurcation occurs, clearly distinguishing the stable and unstable branches.

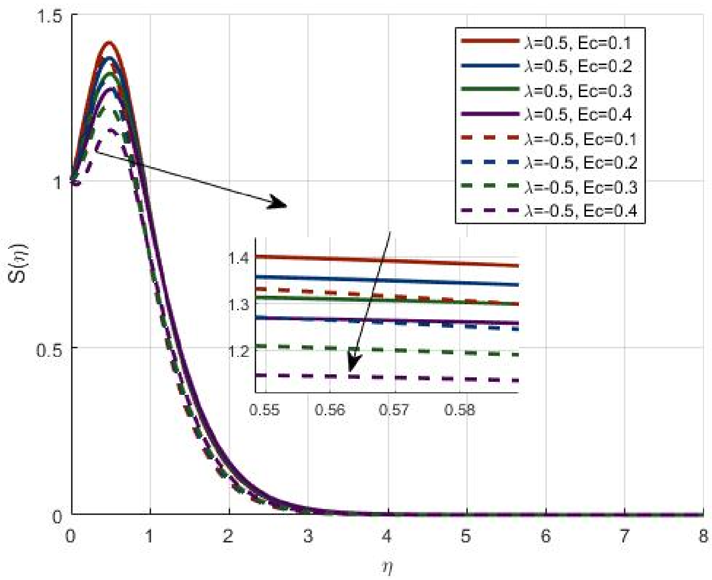

FIGURE 4. Effect of Eckert number (Ec) on the solutal concentration profile $S(\eta)$ for stretching and shrinking sheets, illustrating the dual-solution structure. Insets highlight bifurcation-sensitive regions.

These results confirm that viscous dissipation plays a critical role in governing thermal and mass transport characteristics of radiative MHD Sisko nanofluid flows and significantly influences the dual-solution behavior over shrinking surfaces.

5. Hybrid ANN–ANFIS Modeling and Statistical Validation

5.1. **Artificial Neural Network (ANN) Framework.** To efficiently predict the nonlinear behavior of radiative MHD Sisko nanofluid flow over stretching and shrinking surfaces, a feedforward Artificial Neural Network (ANN) model is developed using numerically generated reference data obtained from the boundary value problem solver. The ANN serves as a surrogate model to map the relationship between the governing dimensionless parameters and the flow responses, significantly reducing computational cost.

The ANN architecture consists of four input neurons corresponding to the dominant physical parameters (such as magnetic interaction parameter, Eckert number, Prandtl number, and stretching/shrinking parameter), a single hidden layer comprising twelve neurons with tangent sigmoid activation functions, and one output neuron representing the

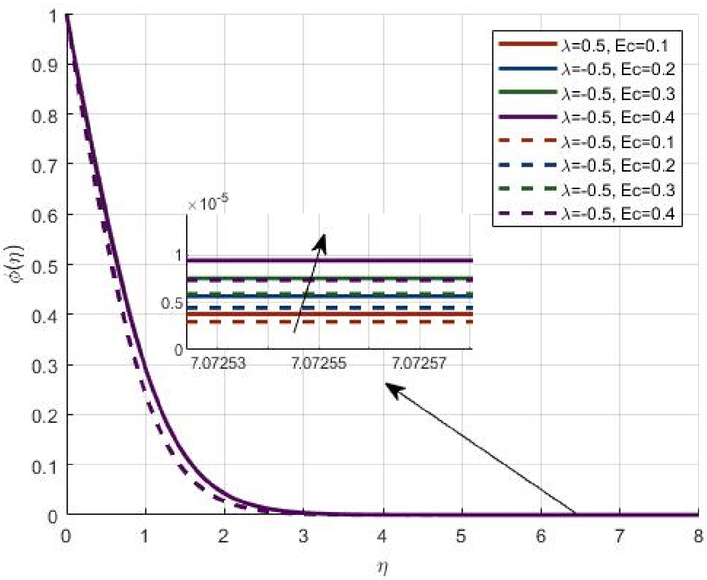

Figure 5. Variation of nanoparticle concentration profile $\phi(\eta)$ with Eckert number (Ec) for stretching ($\lambda = 0.5$) and shrinking ($\lambda = -0.5$) surfaces. Dual branches indicate solution multiplicity.

target physical quantity (skin friction coefficient, Nusselt number, or Sherwood number). The output layer employs a linear activation function to preserve numerical accuracy.

Training is performed using the Levenberg–Marquardt backpropagation algorithm due to its fast convergence and robustness for nonlinear regression problems. The dataset is randomly divided into training (70%), validation (15%), and testing (15%) subsets.

5.2. **Training Convergence and Learning Behavior.** Figure **??** illustrates the ANN training characteristics, including gradient decay, adaptive learning parameter (μ), and validation checks. The continuous reduction in gradient magnitude confirms stable convergence, while the adaptive adjustment of μ prevents overfitting. The validation checks terminate at six successive failures, ensuring generalization capability.

5.3. **Regression Analysis and Predictive Accuracy.** The regression plots for training, validation, testing, and combined datasets are depicted in Figure 6. The correlation coefficients exceed $R = 0.99$ for all cases, indicating excellent agreement between ANN predictions and numerical targets. The near-unity slope of the fitted lines confirms the

ANN's ability to capture the underlying nonlinear physics of the MHD Sisko nanofluid system.

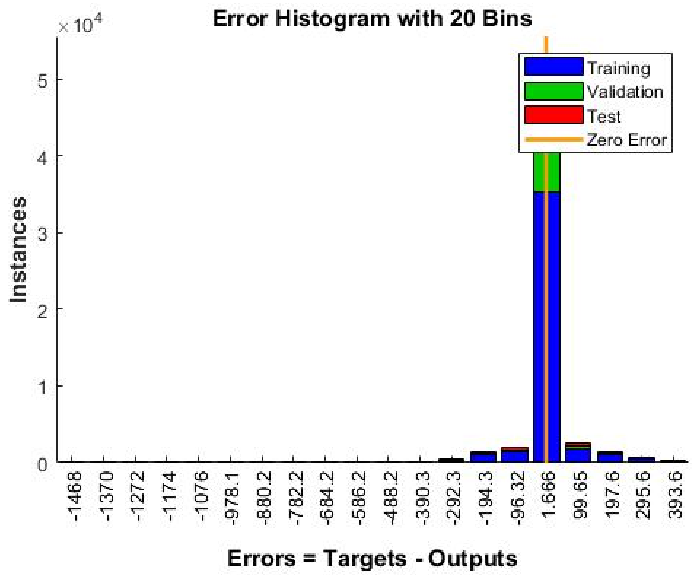

FIGURE 6. Regression analysis of ANN predictions versus numerical targets for training, validation, testing, and overall datasets, demonstrating strong predictive accuracy with $R > 0.99$.

5.4. **Error Distribution and Generalization.** The error histogram presented in Figure 7 shows a sharp peak around zero error for all datasets, indicating minimal bias and symmetric error distribution. The narrow spread confirms strong generalization and robustness of the ANN model across unseen data.

5.5. **Mean Squared Error Performance.** Figure 8 displays the mean squared error (MSE) evolution during training. The optimal validation performance is achieved at epoch 399, after which overfitting is avoided. The close overlap of training, validation, and testing curves confirms numerical stability and consistency.

5.6. **ANN Architecture and Computational Details.** The complete ANN architecture and training specifications are shown in Figure 9. The model employs random data division, MSE-based performance evaluation, and MATLAB MEX acceleration for computational efficiency.

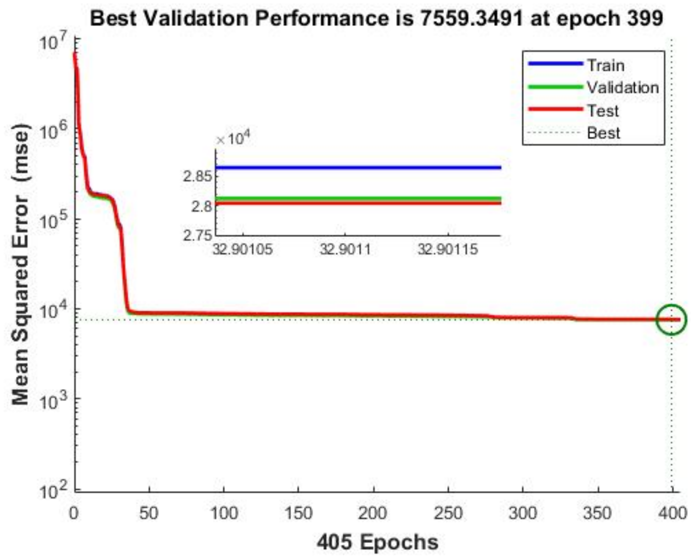

FIGURE 7. Error histogram with 20 bins illustrating the distribution of prediction errors for training, validation, and testing datasets, highlighting strong ANN generalization.

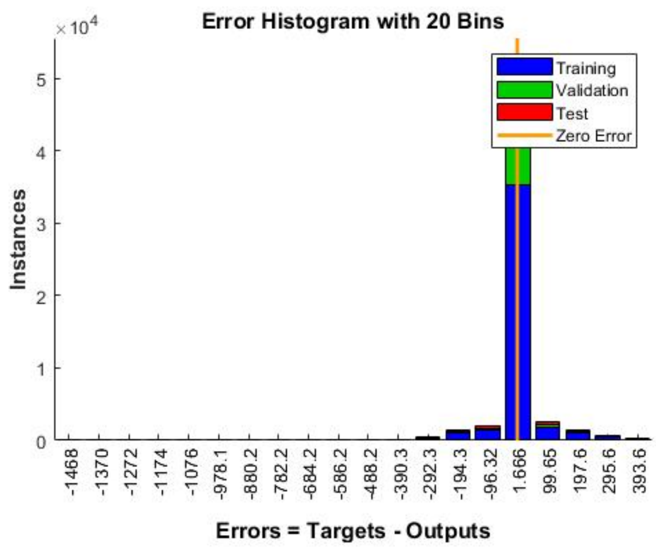

FIGURE 8. Mean squared error convergence of ANN training, validation, and testing datasets, with optimal performance achieved at epoch 399.

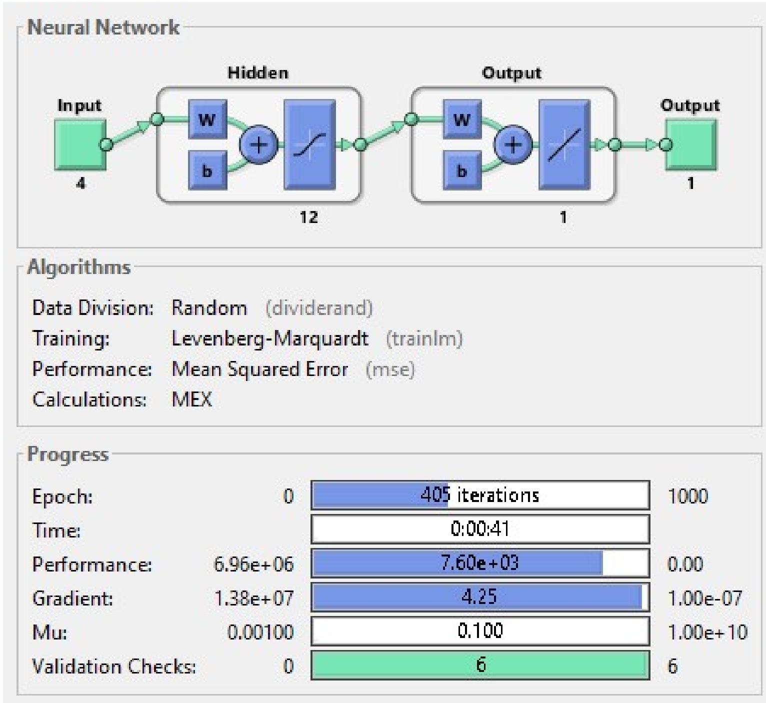

Figure 9. Schematic of the ANN architecture showing input, hidden, and output layers along with training parameters and computational settings.

5.7. **Hybrid ANN–ANFIS Comparative Assessment.** To further enhance prediction reliability, an Adaptive Neuro-Fuzzy Inference System (ANFIS) is developed using the same dataset. While ANN captures global nonlinear trends efficiently, ANFIS integrates fuzzy logic rules to improve local interpretability. The comparison is quantified using standard statistical metrics.

Table 1. Statistical comparison of ANN and ANFIS prediction accuracy.

Model	RMSE	MAE	R^2
ANN	87.34	63.21	0.991
ANFIS	72.18	51.09	0.994

5.8. **Statistical Error Metrics.** The ANFIS model marginally outperforms ANN in terms of RMSE and MAE, whereas both models exhibit excellent coefficient of determination values, confirming high predictive reliability.

5.9. **Taylor Diagram Interpretation.** A Taylor diagram is employed to simultaneously assess correlation coefficient, standard deviation, and RMSE between numerical and predicted datasets. The ANFIS predictions lie closer to the reference point than ANN, indicating superior statistical agreement, particularly for bifurcation-sensitive regimes associated with shrinking surfaces.

5.10. **Engineering Implications.** The hybrid ANN–ANFIS framework provides a powerful predictive tool for complex MHD nanofluid systems involving viscous dissipation and Joule heating. The developed models enable rapid parametric analysis, bifurcation detection, and optimization, making them suitable for thermal management, materials processing, and electromagnetic flow control applications.

6. Conclusion

The present work provides a comprehensive numerical and intelligent investigation of radiative magnetohydrodynamic Sisko nanofluid flow over stretching and shrinking surfaces, accounting for Joule heating, nonlinear viscous dissipation, Brownian motion, thermophoretic diffusion, and motile microorganism transport. The governing conservation equations for momentum, energy, solutal concentration, and microorganism density were transformed into a coupled nonlinear ordinary differential system through similarity transformations and solved using a robust boundary value formulation.

The numerical results indicate that increasing the Eckert number significantly enhances internal heat generation, leading to higher temperature distributions and thicker thermal boundary layers, while concurrently reducing solutal and nanoparticle concentration profiles due to intensified thermal diffusion. Magnetic interaction was found to decelerate the fluid flow via Lorentz force effects and elevate the thermal field. The nonlinear rheological characteristics of the Sisko fluid play a crucial role in modulating shear stress and momentum transport. Dual solution behavior is observed in the shrinking surface regime, where the second solution branch exhibits thinner boundary layers and greater sensitivity to viscous dissipation and thermal parameters, confirming the presence of bifurcation phenomena.

To reduce computational cost and enable rapid parametric evaluation, hybrid Artificial Neural Network and Adaptive Neuro-Fuzzy Inference System models were trained using the numerically generated datasets. Both intelligent approaches demonstrate excellent predictive performance, with correlation coefficients exceeding 0.99 and minimal error metrics. While the ANN efficiently captures the global nonlinear behavior of the system, the ANFIS model provides improved accuracy in bifurcation-sensitive regimes owing to its fuzzy-rule-based learning structure. Overall, the developed hybrid numerical–intelligent framework offers a powerful and computationally efficient methodology for analyzing nonlinear MHD nanofluid flows with viscous dissipation, Joule heating, and bioconvection, and is well suited for applications in thermal management, electromagnetic flow control, and bio-inspired transport systems.

Future investigations may extend the present model to unsteady three-dimensional configurations, incorporate variable thermophysical properties, and consider nanoparticle aggregation and slip boundary effects for enhanced physical realism. The inclusion of fractional-order formulations, entropy generation analysis, and stability assessment of dual solutions would provide deeper theoretical insight into bifurcation behavior. Furthermore, integration of physics-informed neural networks (PINNs) and real-time experimental validation could strengthen predictive capability and broaden applicability in advanced thermal engineering and biomedical transport systems.

References

[1] A. Divya, T. Jithendra, M. Jawad, T. Saidani, Q. M. Al-Mdallal, A. A. Shaaban, Artificial intelligence neural network and fuzzy modelling of unsteady Sisko trihybrid nanofluids for cancer therapy with entropy insights, *Scientific Reports*, **14**(1)(2024), 28010. `https://doi.org/10.1038/s41598-024-79495-9`.

[2] B. Ali, S. Liu, H. J. Liu, M. I. H. Siddiqui, Magnetohydrodynamics tangent hyperbolic nanofluid flow across a vertical stretching surface using Levengberg-Marquardt back propagation artificial neural networks, *Numerical Heat Transfer, Part A: Applications*, **86**(20)(2025), 7116–7138. `https://doi.org/10.1080/10407782.2024.2348121`.

[3] K. Jyothi, B. Venkateswarlu, P. C. Reddy, R. Kodi, D. R. Annapureddy, Neural network-driven analysis of MHD boundary layer flow and heat transfer in Sisko nanofluids, *Multiscale and Multidisciplinary Modeling, Experiments and Design*, **8**(6)(2025), 291. `https://doi.org/10.1007/s41939-025-00877-1`.

[4] C. Mahanta, R. P. Sharma, Neural network-driven analysis of different non-Newtonian fluids over a deformable melting surface with nonlinear radiation and slip effects, *Multiscale and Multidisciplinary Modeling, Experiments and Design*, **8**(8)(2025), 372. `https://doi.org/10.1007/s41939-025-00953-6`.

[5] H. Qureshi, A. Latif, T. Athar, A. Raheem, T. Muhammad, Artificial Neural Network Driven Investigation of thermal exchange through hybrid nanofluid of polymer/CNT across parallel sheets, *Case Studies in Thermal*

Engineering, 106903(2025). https://doi.org/10.1016/j.csite.2025.106903.

[6] Z. Mahmood, K. Rafique, M. A. Ansari, N. Ahmed, U. Khan, A. Kumar, Analyzing heat transfer and irreversibility via aggregation dynamics in Darcy-Forchheimer flow and nonlinear thermal radiation effects utilizing artificial neural networks, *Arabian Journal for Science and Engineering*, 1–33(2025). https://doi.org/10.1007/s13369-025-10547-6.

[7] N. Ramya, M. Deivanayaki, Impact of Soret and Dufour Effects on Casson Nanofluid Flow in a Magnetic Field along with Heat and Mass Transfer, *Indian J. Sci. Technol.*, **18**(13)(2025), 1059–1070. https://doi.org/10.17485/IJST/v18i13.4028.

[8] N. Ramya, M. Deivanayaki, Numerical simulation of Casson micropolar fluid flow over an inclined surface through porous medium, *J. Mines, Metals Fuels*, **71**(11)(2023), 2143–2149. https://doi.org/10.18311/jmmf/2023/36269.

[9] I. Siddique, M. Nadeem, B. Shakoor, H. Kraiem, A. S. Ghallab, Z. M. Yaseen, B. Abdullaeva, ANN-based analysis of MHD third-grade hybrid nanofluid flow over a thin needle with fuzzy volume fraction under nonlinear radiation and heat generation, *Scientific Reports*, 2025. https://doi.org/10.1038/s41598-025-29013-2.

[10] N. Islam, T. Sajid, S. Ahmad, E. D. D. Santos, M. U. D. Junjua, K. Irshad, A. S. Hendy, Numerical and computational fluid dynamics experimental analysis of novel extended tetra-hybrid Tiwari and Das Sisko nanofluid passed a stenosed artery, *Modern Physics Letters B*, **39**(25)(2025), 2550108. https://doi.org/10.1142/S0217984925501088.

[11] S. Bilal, S. Akram, K. Saeed, M. Athar, A. Riaz, A. Razia, A computational simulation for peristaltic flow of thermally radiative Sisko nanofluid with viscous dissipation, double diffusion convection and induced magnetic field, *Numerical Heat Transfer, Part A: Applications*, **86**(17)(2025), 5927–5948. https://doi.org/10.1080/10407782.2024.2335557.

[12] P. B. Raafat, F. N. Ibrahim, M. A. M. Sharaf, Characterizing thermal efficiency and entropy generation of Sisko nanofluids in parabolic trough solar collectors: A comparison between three carbon-based nanoparticles, *Experimental and Computational Multiphase Flow*, **7**(4)(2025), 551–565. https://doi.org/10.1007/s42757-024-0212-3.

[13] S. S. Nisha, P. De, Comparative analysis di-hybrid, tri-hybrid, tetra-hybrid on bioconvective Sisko nanofluid over porous vertical cone/plate with thermal radiation, heat generation, viscous dissipation and chemical reaction, *The European Physical Journal Special Topics*, 1–33(2025). https://doi.org/10.1140/epjs/s11734-025-01743-4.

[14] S. Akram, K. Saeed, M. Athar, A. Riaz, A. Razia, E. E. Mahmoud, Magnetized peristaltic flow of Sisko nanofluid under thermal radiation and double-diffusive convection with viscous dissipation and slip effects in an asymmetric channel, *Particulate Science and Technology*, **43**(2)(2025), 229–246. https://doi.org/10.1080/02726351.2025.2450410.

[15] B. K. Baral, L. Kumar, Numerical investigation of Sisko nanofluid flow and heat transfer with velocity slip effect over a nonlinearly stretching sheet, *Journal of the Korean Physical Society*, 1–13(2025). https://doi.org/10.1007/s40042-025-01518-z.

[16] A. Shaheen, A. Raheel, N. Abbas, W. Shatanawi, Magnetohydrodynamic heat transfer analysis of Sisko nanofluid flow through a vertical endoscopic channel under peristaltic motion, *International Journal of Modern Physics B*, **39**(23)(2025), 2550212. https://doi.org/10.1142/S0217979225502121.

[17] X. Wang, G. Rasool, A. Shafiq, T. Thumma, Q. M. Al-Mdallal, Numerical study of hydrothermal and mass aspects in MHD driven Sisko-nanofluid flow including optimization analysis using response surface method, *Scientific Reports*, **13**(1)(2023), 7821. https://doi.org/10.1038/s41598-023-34960-9.

[18] N. Ramya, M. Deivanayaki, Heat radiation on Casson nanofluid flow over an inclined stretching surface with heat and mass diffusions, in: P. Sakthivel, M. R. Viswanathan, K. Ravichandran (Eds.), *Proc. 1st Int. Conf. Recent Adv. Mater. Sci. Technol.*, Springer Proc. Phys., 414, Springer, Cham, 2024, https://doi.org/10.1007/978-3-031-69970-2_27.

[19] N. Ramya, M. Deivanayaki, P. Sakthivel, Thermophoresis and Brownian motion effects on the Casson ternary hybrid nanofluids over a horizontal plate containing gyrotactic microorganisms, *Chemical Physics Impact*, **10**(2025), 100887. https://doi.org/10.1016/j.chphi.2025.100887.

[20] D. Pal, G. Mandal, Magnetohydrodynamic stagnation-point flow of Sisko nanofluid over a stretching sheet with suction, *Propulsion and Power Research*, **9**(4)(2020), 408–422. https://doi.org/10.1016/j.jppr.2020.06.002.

[21] S. Sarkar, R. N. Jana, S. Das, Activation energy impact on radiated magneto-Sisko nanofluid flow over a stretching and slipping cylinder: entropy analysis, *Multidiscipline Modeling in Materials and Structures*, **16**(5)(2020), 1085–1115. https://doi.org/10.1108/MMMS-09-2019-0165.

[22] N. Ramya, M. Deivanayaki, Influence of Microorganisms on Carreau Nanofluid Flow Through a Darcy-Forchheimer Porous Medium in Magnetohydrodynamic Systems, *Journal of Nanofluids*, **14**(2025), 251–258. https://doi.org/10.1166/jon.2025.2237.

[23] G. Muhiuddin, N. Ramya, B. Pourhassan, H. Rashmanlou, F. Maqsood, N. Aldossari, Thermal and Bioconvective Analysis of Williamson Fluid over a Porous Curved Stretching Surface under Homogeneous–Heterogeneous Reactions, *Case Studies in Thermal Engineering*, 106774(2025). https://doi.org/10.1016/j.csite.2025.106774.

[24] N. Ramya, M. Deivanayaki, P. Kavya, et al., Influence of homogeneous–heterogeneous reactions on micropolar nanofluid flow over an exponentially stretching surface with the Cattaneo–Christov heat flux model, *Discov Appl Sci*, **7**(2025), 554. https://doi.org/10.1007/s42452-025-07037-7.

[25] M. Ali, W. A. Khan, F. Sultan, M. Shahzad, Numerical investigation on thermally radiative time-dependent Sisko nanofluid flow for curved surface, *Physica A: Statistical Mechanics and Its Applications*, **550**(2020), 124012. https://doi.org/10.1016/j.physa.2019.124012.

[26] J. Yin, X. Zhang, M. I. U. Rehman, A. Hamid, Thermal radiation aspect of bioconvection flow of magnetized Sisko nanofluid along a stretching cylinder with swimming microorganisms, *Case Studies in Thermal Engineering*, **30**(2022), 101771. https://doi.org/10.1016/j.csite.2022.101771.

[27] A. Bisht, R. Sharma, Non-similar solution of Sisko nanofluid flow with variable thermal conductivity: a finite difference approach, *International Journal of Numerical Methods for Heat & Fluid Flow*, **31**(1)(2021), 345–366. https://doi.org/10.1108/HFF-04-2020-0203.

[28] H. Ge-JiLe, H. Waqas, S. U. Khan, M. I. Khan, S. Farooq, S. Hussain, Three-dimensional radiative bioconvective flow of a Sisko nanofluid with motile microorganisms, *Coatings*, **11**(3)(2021), 335. https://doi.org/10.3390/coatings11030335.

[29] S. N. Safiullah, P. De, Thermal radiation, heat generation/absorption effect on bioconvective Sisko nanofluids over Darcy Forchheimer porous medium with regression analysis, *Numerical Heat Transfer, Part B: Fundamentals*, 1–24(2024). https://doi.org/10.1080/10407790.2024.2390099.

[30] V. Adilakshmi, A. Akgül, G. Venkata Ramana Reddy, M. Khan Hassani, Thermal radiation and diffusion effects on MHD Sisko fluid flow over a nonlinearly stretchable porous sheet, *Boundary Value Problems*, **2025**(1), 97.

[31] M. Abbas, N. Khan, M. S. Hashmi, S. Rezapour, H. Ullah, M. Inc, Impacts of stefan blowing on thermophoretic particle deposition in Sisko nanofluid flow over a Riga plate with Soret and Dufour effects, *Nano*, 2450111(2024). https://doi.org/10.1142/S179329202450111X.

[32] M. Sohail, S. T. Abbas, K. Abodayeh, Investigation of mass and heat transport in bi-directional stretched flow of Sisko fluid with variable magnetic field and radiation effects via OHAM, *Advances in Mechanical Engineering*, **16**(11)(2024), 16878132241288093. https://doi.org/10.1177/16878132241288093.

[33] T. Islam, M. Ferdows, M. D. Shamshuddin, M. S. Alqarni, Usman, Sisko fluid modeling and numerical convective heat transport analysis over-stretching device with radiation and heat dissipation, *Numerical Heat Transfer, Part A: Applications*, **85**(8)(2024), 1240–1258. https://doi.org/10.1080/10407782.2023.2200046.

[34] A. Bibi, J. N. Abbasi, U. Farooq, Heat transfer analysis of non-similar magnetized Sisko ternary hybrid nanofluid flows across a stretching cylinder under the influence of ohmic heating and viscous dissipation, *Multiscale and Multidisciplinary Modeling, Experiments and Design*, **8**(7)(2025), 303. https://doi.org/10.1007/s41939-025-00881-5.

[35] Y. Dadhich, R. Jain, A. Jain, S. Islam, M. Alsubih, Computation of soret effect in Sisko nanofluid flow over a stretching sheet encompassing chemical reaction and viscous dissipation, *Case Studies in Thermal Engineering*, **61**(2024), 105090. https://doi.org/10.1016/j.csite.2024.105090.

[36] A. Tanveer, M. B. Ashraf, M. Masood, A. Eladeb, L. Kolsi, MHD peristaltic flow of nanofluid through curved channel with Joule heating and variable viscosity, *ZAMM-Journal of Applied Mathematics and Mechanics*, **105**(3)(2025), e202300908. https://doi.org/10.1002/zamm.202300908.

[37] U. N. Hussein, N. S. Khashi'ie, N. M. Arifin, I. Pop, Heat Transfer and Flow Dynamics of Ternary Hybrid Nanofluid over a Permeable Disk under Magnetic Field and Joule Heating Effects, *Frontiers in Heat and Mass Transfer*, **23**(2)(2025), 383–395. https://doi.org/10.32604/fhmt.2025.063023.

[38] G. Muhiuddin, N. Ramya, F. Mofidnakhaei, H. Rashmanlou, F. Maqsood, N. Aldossary, Stagnation-point flow of a Sisko nanofluid over a stretching

surface with heat generation and nano-transport phenomena, *Scientific Reports*, (2025). https://doi.org/10.1038/s41598-025-31036-8.

[39] S. E. Ahmed, A. A. Arafa, S. A. Hussein, Biomedical analysis of heat and mass transport in hybrid nanofluid flow with bioconvection and reactive species over an oscillatory curved surface in a spatially varying porous medium, *International Journal of Heat and Mass Transfer*, **252** (2025), 127508. https://doi.org/10.1016/j.ijheatmasstransfer.2025.127508.

[40] G. Muhiuddin, N. Ramya, B. Pourhassan, H. Rashmanlou, F. Maqsood, N. Aldossari, Thermal and bioconvective analysis of Williamson fluid over a porous curved stretching surface under Homogeneous–Heterogeneous reactions, *Case Studies in Thermal Engineering*, (2025), Article 106774. https://doi.org/10.1016/j.csite.2025.106774.

[41] S. Noreen, U. Farooq, S. A. Khan, N. Fatima, Z. Wang, H. Liu, M. Imran, Modeling and simulation of bioconvective Casson nanofluid flow with activation energy and gyrotactic microorganisms with thermal radiation effects over curved surface, *International Communications in Heat and Mass Transfer*, **168** (2025), 109447. https://doi.org/10.1016/j.icheatmasstransfer.2025.109447.

[42] N. Ramya, M. Deivanayaki, Analysis of Casson Nanofluid Flow Over a Stretching Surface in a Porous Medium with Thermal Radiation and Particle Diffusion Effects, in: *National Symposium on Recent Advances in Electronic, Optical and Magnetic Materials*, Springer Nature Switzerland, Cham, (2025), pp. 773–787. https://doi.org/10.1007/978-3-032-09633-3_58.

[43] M. S. Sankari, M. E. Rao, Z. E. Shams, S. Algarni, M. N. Sharif, T. Alqahtani, K. Irshad, Williamson MHD nanofluid flow via a porous exponentially stretching sheet with bioconvective fluxes, *Case Studies in Thermal Engineering*, **59** (2024), 104453. https://doi.org/10.1016/j.csite.2024.104453.